PHYSICAL REVIEW B VOLUME 24, NUMBER 10 15 NOVEMBER 1981

Retarded edge modes of a parabolic wedge

A. D. Boardman
Department of Pure and Applied Physics, University of Salford, Salford, M5 4WT United Kingdom

G. C. Aers*
Department of Pure and Applied Physics, University of Salford, Salford, M5 4WT United Kingdom and Theoretical Physics Institute, The University of Alberta, Edmonton, T6G 2J1 Canada

R. Teshima
Theoretical Physics Institute, The University of Alberta, Edmonton, T6G 2J1 Canada
(Received 2 March 1981)

The dispersion of the retarded edge modes of a free-electron—metal parabolic wedge is determined. It is shown that, although the modes are decoupled within the electrostatic approximation, decoupling does not occur when the full set of Maxwell's equations is used. This feature is considered in detail and a novel solution is given, together with some numerical examples. It is shown that the dispersion equation is in the form of an infinite determinant that can be arranged in block diagonal form. The method depends upon certain expansion coefficients that, through a completely new mathematical result concerning Hermite functions, are shown to have a closed form. The validity of labeling the eigenmodes is discussed, and the convergence of the solution scheme is carefully examined. It is found that the retarded modes are quite close to the electrostatic modes, even as the light line is approached, with maximum disparity arising for the odd mode numbers.

I. INTRODUCTION

In principle, a dielectric wedge should permit the existence of electromagnetic waves that are localized within the vicinity of the sharp edge and propagating freely along it. In a previous study Dobrzynski and Maradudin[1] showed that electrostatic modes of this type indeed exist but have frequencies that are independent of wave number and depend continuously on the Laplace-equation separation constant. Davis[2] has considered the electrostatic modes of a hyperbolic cylinder and has concluded that the Dobrzynski and Maradudin[1] results are associated with the sharpness of the edge of the wedge.

The use of a hyperbolic cylinder is quite a good idea since the sharp-edged wedge is its natural limit. An effect equivalent to the rounding of the edge of the wedge can also be achieved by using a nonlocal dielectric function.[3] An alternative system that supports edge modes, but does not have the sharp edge as a limit, is the parabolic cylinder. This was first studied, within the electrostatic approximation, by Eguiluz and Maradudin.[4]

For an electrostatic approximation, the modes are decoupled, leading to a considerable simplification in their treatment.[4] Retarded modes, however, involve the full set of Maxwell's equations with the result that such a decoupling does not occur. This feature is considered in some detail in this paper and a novel solution is given together with some numerical examples. It is shown that the dispersion equation is in the form of a product of two infinite determinants and that although the solutions of each one are, strictly speaking, coupled together, they can be precisely labeled.

In Sec. II the field equations are derived and the total field is expressed in terms of linear combinations of electric (E) waves and magnetic (B) waves. In Sec. III it is shown, by an expansion techinque, that separate dispersion relations for even- and odd-order coupled modes can be produced. Section IV contains details of the numerical method of solution and the relationship of the results to the electrostatic modes. The Appendix contains what we believe to be a completely new mathematical result concerning harmonic oscillator eigenfunctions.

II. FIELD EQUATIONS

We consider the parabolic cylinder shown in Fig. 1 and use the standard coordinates (ξ,η,z) where the

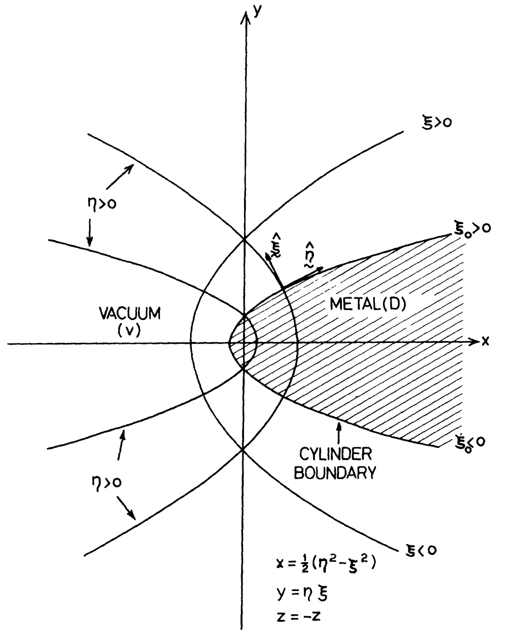

FIG. 1. Parabolic cylinder coordinates. The z axis is perpendicular to the figure. The boundary between dielectric and vacuum is given by $|\xi| = |\xi_0|$. The dielectric occupies the region $|\xi| \leq |\xi_0|$.

z axis is normal to the plane of the figure. The dielectric, in this case a free-electron plasma representing a metal with dielectric function ϵ_D, occupies the region $|\xi| < |\xi_0|$ and the vacuum with the dielectric function $\epsilon_V = 1$ occupies the region $|\xi| > |\xi_0|$.

As expected from studies of the circular cylinder,[5,6] the total field does not decouple into E- and B-wave solutions but is a linear combination of both. For an E-wave solution $B_z = 0$ and the axial electric field component satisfies

$$(\nabla^2 - \alpha_{D,V}^2)E_z = 0 , \tag{1}$$

where

$$\alpha_{D,V}^2 = -\epsilon_{D,V}\frac{\omega^2}{c^2} \tag{2}$$

and the subscripts D and V denote dielectric and vacuum, respectively. The edge-mode field solutions are of the form $f(\xi,\eta)\exp[i(qz-\omega t)]$, where $\vec{q}$ is the axial wave vector. Hence Eq. (1), in parabolic cylinder coordinates, is

$$\frac{\partial^2 E_z}{\partial \xi^2} + \frac{\partial^2 E_z}{\partial \eta^2} - F_{D,V}^2 \Delta^2 E_z = 0 , \tag{3}$$

where

$$F_{D,V}^2 = \alpha_{D,V}^2 + q^2 , \tag{4}$$

$$\Delta^2 = \eta^2 + \xi^2 . \tag{5}$$

Equation (3), through the introduction of a separation constant I, is equivalent to the two equations

$$\frac{\partial^2 E_z}{\partial \eta^2} + (I - F_{D,V}^2\eta^2)E_z = 0 , \tag{6}$$

$$\frac{\partial^2 E_z}{\partial \xi^2} - (I + F_{D,V}^2\xi^2)E_z = 0 . \tag{7}$$

Equation (6) has a solution $\mathscr{H}_n(F_{D,V}^{1/2}\eta)$, which is the familiar eigenfunction of the harmonic oscillator,[7] i.e., the Hermite function

$$\mathscr{H}_n(F_{D,V}^{1/2}\eta) = e^{-F_{D,V}\eta^2/2}H_n(F_{D,V}^{1/2}\eta)/(2^n n!\sqrt{\pi})^{1/2} \tag{8}$$

where H_n is a Hermite polynomial and $I = (2n+1)F_{D,V}$. If we take $\chi = \xi(2F_{D,V})^{1/2}$, then Eq. (7) can be written as

$$\frac{\partial^2 E_z}{\partial \chi^2} - \left[n + \frac{1}{2} + \frac{\chi^2}{4}\right]E_z = 0 , \tag{9}$$

whose solutions are the parabolic cylinder functions[8(a)] $V(n+\frac{1}{2},(2F_D)^{1/2}\xi)$ for $\xi \leq \xi_0$ and $U(n+\frac{1}{2},(2F_V)^{1/2}\xi)$ for $\xi \geq \xi_0$, chosen to have the correct behavior as $\xi \to 0,\infty$. The general form of E_z is therefore

$$E_z = e^{i(qz-\omega t)}\sum_n \begin{cases} A_n\mathscr{H}_n(Y_D)V_n(X_D), & \xi \leq \xi_0 \\ C_n\mathscr{H}_n(Y_V)U_n(X_V), & \xi \geq \xi_0 \end{cases} \tag{10}$$

where $Y_{D,V} = F_{D,V}^{1/2}\eta$, $X_{D,V} = (2F_{D,V})^{1/2}\xi$, $V_n(X_D) = V(n+\frac{1}{2},X_D)$, and $U_n(X_V) = U(n+\frac{1}{2},X_V)$.

The axial magnetic field required to construct the B-wave solutions is, by similar reasoning,

$$B_z = e^{i(qz-\omega t)}\sum_n \begin{cases} B_n\mathscr{H}_n(Y_D)V_n(X_D), & \xi \leq \xi_0 \\ D_n\mathscr{H}_n(Y_V)U_n(X_V), & \xi \geq \xi_0 . \end{cases} \tag{11}$$

From Maxwell's equations, after suppressing the z and t dependence since it is common to all components, the relevant field components of the two field types are

$$E_z = \begin{cases} \sum_n \begin{cases} A_n\mathscr{H}_n(Y_D)V_n(X_D) \\ C_n\mathscr{H}_n(Y_V)U_n(X_V) \end{cases} \text{for } E \text{ waves} \\ 0 \text{ for } B \text{ waves} , \end{cases}$$

$$E_\eta = \begin{cases} -\dfrac{iq}{\Delta}\sum\limits_n \begin{cases} A_n F_D^{-3/2}\mathscr{H}_n'(Y_D)V_n(X_D) \\ C_n F_V^{-3/2}\mathscr{H}_n'(Y_V)U_n(X_V) \end{cases} \text{for } E \text{ waves} \\ \dfrac{i\omega\sqrt{2}}{\Delta}\sum\limits_n \begin{cases} B_n F_D^{-3/2}\mathscr{H}_n(Y_D)V_n'(X_D) \\ D_n F_V^{-3/2}\mathscr{H}_n(Y_V)U_n'(X_V) \end{cases} \text{for } B \text{ waves}, \end{cases}$$

$$B_z = \begin{cases} 0 \text{ for } E \text{ waves} \\ \sum\limits_n \begin{cases} B_n \mathscr{H}_n(Y_D)V_n(X_D) \\ D_n \mathscr{H}_n(Y_V)U_n(X_V) \end{cases} \text{for } B \text{ waves}, \end{cases} \tag{12}$$

$$B_\eta = \begin{cases} \dfrac{i\sqrt{2}}{\omega\Delta}\sum\limits_n \begin{cases} A_n \alpha_D^2 F_D^{-3/2}\mathscr{H}_n(Y_D)V_n'(X_D) \\ C_n \alpha_V^2 F_V^{-3/2}\mathscr{H}_n(Y_V)U_n'(X_V) \end{cases} \text{for } E \text{ waves} \\ -\dfrac{iq}{\Delta}\sum\limits_n \begin{cases} B_n F_D^{-3/2}\mathscr{H}_n'(Y_D)V_n(X_D) \\ D_n F_V^{-3/2}\mathscr{H}_n'(Y_V)U_n(X_V) \end{cases} \text{for } B \text{ waves}, \end{cases}$$

where the prime denotes differentiation with respect to the argument. The actual total field components are obtained by adding together the E- and B-wave contributions.

III. THE EDGE-MODE DISPERSION EQUATION

Since spatial dispersion is being neglected, only four boundary conditions are required involving the continuity of tangential electric and magnetic fields. These can be written as

$$[E_\eta]_{\xi_0} = 0, \quad [E_z]_{\xi_0} = 0, [B_\eta]_{\xi_0} = 0, \quad [B_z]_{\xi_0} = 0, \tag{13}$$

where $[C]_{\xi_0}$ represents the change in a quantity C on the boundary $\xi = \xi_0$. Canceling common factors and writing $V_n^0 = V(n+\frac{1}{2},(2F_D)^{1/2}\xi_0)$, $U_n^0 = U(n+\frac{1}{2},(2F_V)^{1/2}\xi_0)$, and $R = (F_D/F_V)^{3/2}$ we obtain the equations

$$\sum_n \{ -q[A_n\mathscr{H}_n'(Y_D)V_n^0 - C_n\mathscr{H}_n'(Y_V)U_n^0R] + \sqrt{2}\omega[B_n\mathscr{H}_n(Y_D)V_n^{0\prime} - D_n\mathscr{H}_n(Y_V)U_n^{0\prime}R]\} = 0, \tag{14}$$

$$\sum_n [A_n\mathscr{H}_n(Y_D)V_n^0 - C_n\mathscr{H}_n(Y_V)U_n^0] = 0, \tag{15}$$

$$\sum_n \left[\frac{\sqrt{2}}{\omega}[A_n\alpha_D^2\mathscr{H}_n(Y_D)V_n^{0\prime} - C_n\alpha_V^2\mathscr{H}_n(Y_V)U_n^{0\prime}] - q[B_n\mathscr{H}_n'(Y_D)V_n^0 - D_n\mathscr{H}_n'(Y_V)U_n^0R] \right] = 0, \tag{16}$$

$$\sum_n [B_n\mathscr{H}_n(Y_D)V_n^0 - D_n\mathscr{H}_n(Y_V)U_n^0] = 0. \tag{17}$$

At this stage it can be seen that this problem is somewhat unusual, because the equations still retain both ξ and η dependence. One or the other of these variables would play the role of the angular term in the circular cylinder case and would be eliminated when the boundary conditions are applied. The way out of this difficulty is to expand $\mathscr{H}_n(Y_D)$ in terms of $\mathscr{H}_n(Y_V)$. We write this expansion as

$$\mathscr{H}_n(Y_D) = \sum_m a_{m,n}\mathscr{H}_m(Y_V). \tag{18}$$

Hence using the orthogonality relationship

$$\int_{-\infty}^{+\infty} \mathscr{H}_m(Y_V)\mathscr{H}_n(Y_V)dY_V = \delta_{m,n} \tag{19}$$

we have

$$a_{m,n}=\int_{-\infty}^{+\infty}\mathcal{H}_m(Y_V)\mathcal{H}_n(Y_D)dY_V\ . \tag{20}$$

The Hermite functions also satisfy the recurrence relationship[7]

$$\mathcal{H}_n'(Y)=\left[\frac{n}{2}\right]^{1/2}\mathcal{H}_{n-1}(Y)-\left[\frac{n+1}{2}\right]^{1/2}\mathcal{H}_{n+1}(Y)\ . \tag{21}$$

Equation (14), after using Eqs. (18), (19), and (21), becomes

$$\sum_n\sum_l\left[-A_nV_n^0[n^{1/2}a_{l,n-1}\delta_{lm}-(n+1)^{1/2}a_{l,n+1}\delta_{lm}]+\frac{2\omega}{q}B_nV_n^{0'}a_{l,n}\delta_{l,m}\right]$$
$$=R\sum_n\left[C_nU_n^0[(n+1)^{1/2}\delta_{m,n+1}-n^{1/2}\delta_{m,n-1}]+\frac{2\omega}{q}D_nU_n^{0'}\delta_{mn}\right]\ . \tag{22}$$

Equations (15) to (17) are dealt with in the exactly the same way. Hence the set of equations obtained through the application of the boundary conditions can be expressed as

$$\sum_n\left[-A_nV_n^0[n^{1/2}a_{m,n-1}-(n+1)^{1/2}a_{m,n+1}]+\frac{2\omega}{q}B_nV_n^{0'}a_{m,n}\right]$$
$$=R\left[m^{1/2}C_{m-1}U_{m-1}^0-(m+1)^{1/2}C_{m+1}U_{m+1}^0+\frac{2\omega}{q}D_mU_m^{0'}\right]\ , \tag{23}$$

$$C_mU_m^0=\sum_nA_nV_n^0a_{m,n}\ , \tag{24}$$

$$\sum_n\{2\alpha_D^2A_nV_n^{0'}a_{m,n}-\omega qB_nV_n^0[n^{1/2}a_{m,n-1}-(n+1)^{1/2}a_{m,n+1}]\}$$
$$=R\{2\alpha_V^2C_mU_m^{0'}+\omega q[m^{1/2}D_{m-1}U_{m-1}^0-(m+1)^{1/2}D_{m+1}U_{m+1}^0]\}\ , \tag{25}$$

$$D_mU_m^0=\sum_nB_nV_n^0a_{m,n}\ . \tag{26}$$

The use of Eqs. (24) and (26) to substitute for C_m and D_m in Eqs. (23) and (25) yields coupled equations of the form

$$\sum_n[\lambda_{m,n}A_n+\theta_{m,n}B_n]=0\ ,\qquad \sum_n[\phi_{m,n}A_n+\lambda_{m,n}B_n]=0\ , \tag{27}$$

where

$$\lambda_{m,n}=\{(n+1)^{1/2}a_{m,n+1}-n^{1/2}a_{m,n-1}+R[(m+1)^{1/2}a_{m+1,n}-m^{1/2}a_{m-1,n}]\}\ ,$$
$$\theta_{m,n}=\frac{2\omega}{q}a_{m,n}\left[\frac{V_n^{0'}}{V_n^0}-R\frac{U_m^{0'}}{U_m^0}\right]\ , \tag{28}$$
$$\phi_{m,n}=\frac{2a_{m,n}}{\omega q}\left[\alpha_D^2\frac{V_n^{0'}}{V_n^0}-\alpha_V^2R\frac{U_n^{0'}}{U_n^0}\right]\ .$$

Note that $a_{m-1,n}=0$ for $m=0$ and $a_{m,n}=0$ if m and n have opposite parity. $a_{m,n}$ is shown in the Appendix to have the closed form

$$a_{m,n}=\left[\frac{m!}{n!}\right]^{1/2}(-1)^{(m-n/2)}P_{(n+m/2}^{(n-m)/2}\left[\frac{2R^{1/3}}{R^{2/3}+1}\right]\left[\frac{2F_V}{F_V+F_D}\right]^{1/2}\ , \tag{29}$$

where P_j^l is an associated Legendre function. This result simplifies $\lambda_{m,n}$ to[9]

$$\lambda_{m,n} = 2(R^{2/3}-1)(n^{1/2}a_{m,n-1} - R^{1/3}m^{1/2}a_{m-1,n}) . \qquad (30)$$

Equation (7) in matrix form is

$$\begin{bmatrix} 0 & \theta_{00} & \lambda_{01} & 0 & 0 & \theta_{02} & \lambda_{03} & 0 & \cdots \\ \phi_{00} & 0 & 0 & \lambda_{01} & \phi_{02} & 0 & 0 & \lambda_{03} & \cdots \\ \lambda_{10} & 0 & 0 & \theta_{11} & \lambda_{12} & 0 & 0 & \theta_{13} & \cdots \\ 0 & \lambda_{10} & \phi_{11} & 0 & 0 & \lambda_{12} & \phi_{13} & 0 & \cdots \\ 0 & \theta_{20} & \lambda_{21} & 0 & 0 & \theta_{22} & \lambda_{23} & 0 & \cdots \\ \phi_{20} & 0 & 0 & \lambda_{21} & \phi_{22} & 0 & 0 & \lambda_{23} & \cdots \\ \lambda_{30} & 0 & 0 & \theta_{31} & \lambda_{32} & 0 & 0 & \theta_{33} & \cdots \\ 0 & \lambda_{30} & \phi_{31} & 0 & 0 & \lambda_{32} & \phi_{33} & 0 & \cdots \\ \vdots & \vdots & \vdots & \vdots & \vdots & \vdots & \vdots & \vdots & \cdots \end{bmatrix} \begin{bmatrix} A_0 \\ B_0 \\ A_1 \\ B_1 \\ A_2 \\ B_2 \\ A_3 \\ B_3 \\ \vdots \end{bmatrix} , \qquad (31)$$

where use has been made of the fact that $a_{m,n}=0$ if m and n have opposite parity. The infinite matrix of Eqs. (31) can be simplified further by noting that interchanging selected rows and columns in its determinant brings it into block diagonal form. The determinant of this diagonal matrix is the product of two infinite determinants, i.e.,

$$\begin{vmatrix} \phi_{00} & \lambda_{01} & \phi_{02} & \lambda_{03} & \cdots \\ \lambda_{10} & \theta_{11} & \lambda_{12} & \theta_{13} & \cdots \\ \phi_{20} & \lambda_{21} & \phi_{22} & \lambda_{23} & \cdots \\ \lambda_{30} & \theta_{31} & \lambda_{32} & \theta_{33} & \cdots \\ \vdots & \vdots & \vdots & \vdots & \end{vmatrix} \begin{vmatrix} \theta_{00} & \lambda_{01} & \theta_{02} & \lambda_{03} & \cdots \\ \lambda_{10} & \phi_{11} & \lambda_{12} & \phi_{13} & \cdots \\ \theta_{20} & \lambda_{21} & \theta_{22} & \lambda_{23} & \cdots \\ \lambda_{30} & \phi_{31} & \lambda_{32} & \phi_{33} & \cdots \\ \vdots & \vdots & \vdots & \vdots & \end{vmatrix} = 0 . \qquad (32)$$

The first determinant yields modes which, as will be shown later, correspond to the even-order modes described in the electrostatic limit by Eguiluz and Maradudin.[4] The second determinant yields modes which correspond to the odd-order modes in that limit. The electrostatic result is recovered in the limit $c\to\infty$ which in Eq. (2) leads to $\alpha_{D,V}\to 0$. Thus $F_{D,V}\to q, R\to 1$, $a_{m,n}\to\delta_{m,n}$ and $\lambda_{m,n}\to 0$. Equation (32) reduces to the result

$$\theta_{mm}\phi_{mm}(c\to\infty) = \left[\frac{V_m^{0'}}{V_m^0} - \frac{U_m^{0'}}{U_m^0}\right]\left[\epsilon_D\frac{V_m^{0'}}{V_m^0} - \frac{U_m^{0'}}{U_m^0}\right] = 0 . \qquad (33)$$

In fact it is the second parenthesis that yields the nontrivial electrostatic result. It turns out that the ϕ_{mm} terms in Eqs. (32) are dominant and can be used to label the roots of this equation despite the fact that the solutions of each determinant are strictly speaking coupled together.

IV. NUMERICAL CALCULATIONS

In the electrostatic limit, $F=1$, and $a_{m,n}=\delta_{m,n}$. If the electrostatic condition is relaxed then although $F>1$ but $a_{m,n}\approx 0$ for values of m and n differing by more than a few orders. That is, the elements of Eq. (32) have rapidly decreasing magnitudes away from the diagonal. This has useful consequences for the solution of these determinants.

Firstly, it might be expected that a reasonable approximation is given by the dominant terms

$$\phi_{mm} = 0 , \qquad (34)$$

which would be expected to behave in a similar fashion to the decoupled electrostatic modes, except for small values of q.

The exact solution of Eq. (32) cannot be separated into decoupled modes because of the finite off-diagonal elements. However, because of the proper-

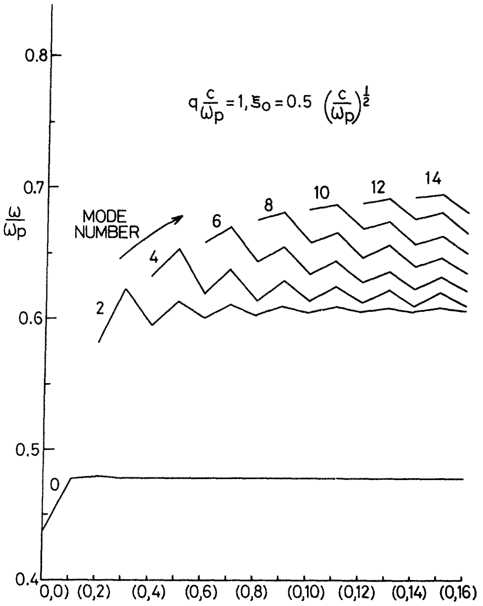

FIG. 2. Convergence of the even-mode solutions of the dispersion equation as function of minimum and maximum row number.

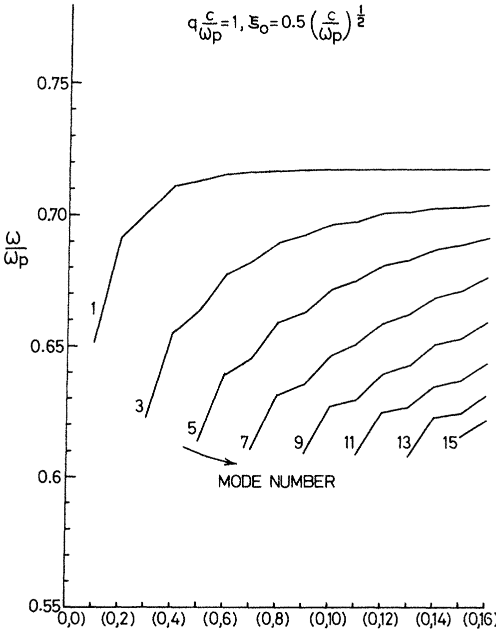

FIG. 3. Convergence of the odd-mode solutions of the dispersion equation as a function of minimum and maximum row number.

ties of $a_{m,n}$, solutions can be found to any desired degree of accuracy by treating modes as being perturbed from the decoupled solutions by the small off-diagonal terms. That is, each solution can be found independently by finding the roots of a determinant containing the ϕ_{mm} term of interest but of increasing magnitude until the result converges. Of course, every second increase in the order of the determinant leads to an additional root due to introduction of a new ϕ_{mm} term. The modes that have the dispersion shown in Figs. 4 and 5 converge satisfactorily for determinants of order 6 to 8 or less.

The convergence properties of the modes is of some interest at this point and these are displayed in Figs. 2 and 3. Even- and odd-mode frequencies are shown for $q = 1$ and $\xi_0 = 0.5$ (focal length of 18 Å for aluminium) measured in units of ω_p/c and $(c/\omega_p)^{1/2}$, as a function of the minimum and maximum row number. Thus (0,3), for example, means the solutions for a 4×4 determinant using rows $0-3$. This means that the solution of the determinant starts at the top left-hand corner and the following sort of progression could be used:

$$\underset{(0,0)}{\phi_{00} = 0}\,, \quad \underset{(0,2)}{\begin{vmatrix} \phi_{00} & \lambda_{01} & \phi_{02} \\ \lambda_{10} & \theta_{11} & \lambda_{12} \\ \phi_{20} & \lambda_{21} & \phi_{22} \end{vmatrix} = 0}\,, \quad \underset{(0,4)}{\begin{vmatrix} \phi_{00} & \cdots & \cdots & \cdots & \cdots \\ \vdots & \phi_{11} & \cdots & \cdots & \cdots \\ \vdots & \vdots & \phi_{22} & \cdots & \cdots \\ \vdots & \vdots & \vdots & \phi_{22} & \cdots \\ \vdots & \vdots & \vdots & \vdots & \phi_{44} \end{vmatrix}} = 0\,. \tag{35}$$

The figures show clearly that a new root emerges as each new ϕ_{mm} is introduced. The following alternative progression could also be used:

$$\begin{vmatrix} \phi_{00} & \lambda_{01} \\ \lambda_{10} & \theta_{11} \end{vmatrix} = 0\,, \quad \begin{vmatrix} \phi_{00} & \cdots & \cdots & \cdots \\ \vdots & \theta_{11} & \cdots & \cdots \\ \vdots & \vdots & \phi_{22} & \cdots \\ \vdots & \vdots & \vdots & \theta_{33} \end{vmatrix} = 0 \tag{36}$$

It is clear that either progression will lead to convergence but the adoption of both results in a zig-zag approach to the convergent result. The modes that have the dispersion shown in Figs. 4 and 5 converge satisfactorily for determinants of order 6 to 8 or less.

Figures 4 and 5 contain the dispersion curves for the first few modes of a free-electron—metal parabolic cylinder with $\epsilon_D = 1 - \omega_p^2\omega^2$ (ω_p is the plasma frequency) and for two values of ξ_0 given by $0.1(c/\omega_p)^{1/2}$ and $0.5(c/\omega_p)^{1/2}$. The eigenfrequency is not plotted as a function of the quantity $\xi_0(2q)^{1/2}$ as was done by Eguiluz and Maradudin[4] since, with the introduction of retardation, this quantity is no longer a universal parameter of the system. The more conventional dimensionless quantity qc/ω_p is used instead. Although the exact solutions are coupled modes we label them for convenience in accordance with the dominant ϕ_{mm} terms in Eq. (32).

In Fig. 4, for the more open structure $\xi_0 = 0.5(c/\omega_p)^{1/2}$, the $m = 0$ and 1 modes obtained from the electrostatic Eq. (33) are shown, together with the solutions that include retardation obtained by the approximate and exact methods described above. All higher modes lie between these modes and, for increasing m, the retarded solutions approach the expected semi-infinite result

$$\epsilon_D F_V + F_D = 0 . \tag{37}$$

This result makes obvious physical sense, and can be seen analytically from the increasing validity of the approximation (34) as m increases. Since, in the limit $m \to \infty$, the terms $V_m^{0'}/V_m^0$ $U_m^{0'}/U_m^0$ approach $(2F_D)^{1/2}$ and $(2F_V)^{1/2}$, respectively, Eq. (36) follows directly.

Figure 4 shows that the approximate solutions suggest that retardation has a stronger effect than it does have in reality. The exact solution tends to remain close to the electrostatic result right down to near the light line, $\omega = qc$, before curving down to a limit asymptotic to this line (note that all electrostatic modes cross the light line and approach $\omega = 0$ or $\omega = \omega_p$ for even and odd modes, respectively, as $q \to 0$).

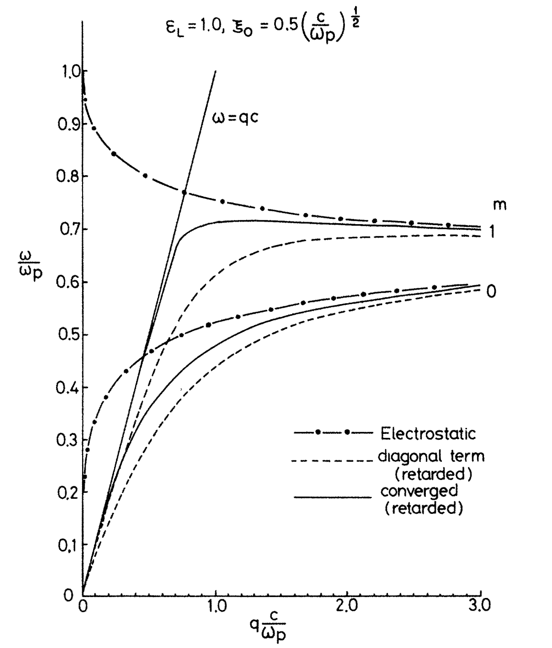

FIG. 4. Dispersion curves for $m = 0$ and $m = 1$ edge modes of a metal parabolic cylinder in vacuum with $\xi_0 = 0.5(c/\omega_p)^{1/2}$. The curve labeled diagonal uses only the first approximation to the eigenvalues. The exact coupled solutions are labeled for convenience by the dominant mode number in their solution.

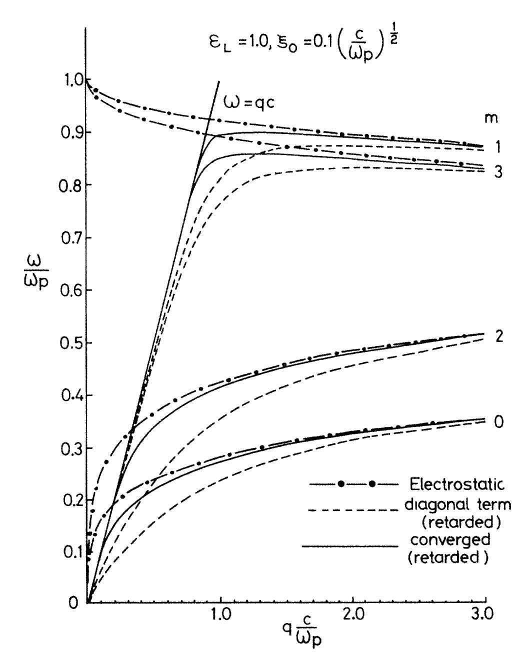

FIG. 5. Dispersion curves for the $m = 0$ to 3 edge modes of a metal parabolic cylinder in vacuum with $\xi_0 = 0.1(c/\omega_p)^{1/2}$. Diagonal is the first approximation to the eigenvalues.

Similar results are obtained for the much sharper structure $\xi_0 = 0.1(c/\omega_p)^{1/2}$ shown in Fig. 5. As expected, the modes separate in frequency as ξ_0 is decreased but once again the electrostatic result is a reasonable approximation to the exact retarded result even quite close to the light line.

ACKNOWLEDGMENTS

A. D. Boardman and G. C. Aers wish to acknowledge the Scientific Affairs Division of NATO for providing support grants and B. V. Paranjape of the University of Alberta, Canada for additional support.

APPENDIX

Equation (20) using (8) is

$$a_{m,n} = \frac{\sqrt{F_V}}{(\pi 2^m m! 2^n n!)^{1/2}} \int_{-\infty}^{\infty} e^{-(F_V+F_D)y^2/2} H_m(y\sqrt{F_V}) H_n(y\sqrt{F_D}) dy \ . \tag{A1}$$

If we introduce

$$y = x\left[\frac{2}{F_V+F_D}\right]^{1/2}, \quad f = \left[\frac{F_D}{F_V}\right]^{1/2} = R^{1/3}, \quad a_{m,n} = \left[\frac{2}{F_V+F_D}\right]^{1/2} A_{m,n} \ ,$$

then

$$A_{m,n} = \frac{1}{(2^m m! 2^n n!)^{1/2}} I\left(m,n,\left[\frac{2}{1+f^2}\right]^{1/2}, f\left[\frac{2}{1+f^2}\right]^{1/2}\right), \tag{A2}$$

where

$$I(m,n,a,b) = \frac{1}{\sqrt{\pi}} \int_{-\infty}^{\infty} e^{-x^2} H_m(ax) H_n(bx) dx \ . \tag{A3}$$

Now the generating function for the Hermite polynomials is

$$e^{2x\lambda-\lambda^2} = \sum_{n=0}^{\infty} \frac{\lambda^n}{n!} H_n(x) \ . \tag{A4}$$

Therefore

$$e^{2ax\lambda-\lambda^2+2bx\mu-\mu^2} = \sum_{m=0}^{\infty}\sum_{n=0}^{\infty} \frac{\lambda^m}{m!}\frac{\mu^n}{n!} H_m(ax) H_n(bx) \ . \tag{A5}$$

Integrating both sides of Eq. (A5) gives

$$\sum_{m=0}^{\infty}\sum_{n=0}^{\infty} \frac{\lambda^m}{m!}\frac{\mu^n}{n!} I(m,n,a,b) = \exp[(a^2-1)\lambda^2 + (b^2-1)\mu^2 + 2ab\lambda\mu] \ . \tag{A6}$$

If the exponential on the right-hand side of (A6) is expanded, it becomes

$$G = \sum_{k=0}^{\infty}\sum_{l=0}^{\infty}\sum_{r=0}^{\infty} \frac{(a^2-1)^k}{k!}\frac{(b^2-1)^l}{l!}\frac{(2ab)^r}{r!} \lambda^{2k+r}\mu^{2l+r} \ , \tag{A7}$$

where since $1/k! = 0$ if $k < 0$ all sums can be extended from $-\infty$ to ∞. This step simplifies the manipulation of the sums. The introduction of Kronecker delta functions to (A7) changes G to

$$G = \sum_{k,l,r} \frac{(a^2-1)^k}{k!}\frac{(b^2-1)^l}{l!}\frac{(2ab)^r}{r!} \lambda^m \mu^n \delta_{m,2k+r}\delta_{n,2l+r} \ . \tag{A8}$$

Hence comparing the coefficients of $\lambda^m\mu^n$ in Eq. (A6) and (A8) gives, after doing the sum over r

$$I(m,n,a,b) = m!n! \sum_{k,l} \frac{(a^2-1)^k}{k!}\frac{(b^2-1)^l}{l!}\frac{(2ab)^{n-2l}}{(n-2l)!} \delta_{m,2k-2l+n} \ , \tag{A9}$$

where

$$\delta_{m,2k-2l-n}=\begin{cases}\delta_{l,k+(n-m)/2}, & n-m \text{ even}\\ 0, & n-m \text{ odd}\,.\end{cases}$$

This is true since the equation $m=2k-2l+n$ cannot be satisfied if $(n-m)$ is odd. Therefore $I(m,n,a,b)=0$ if $(n-m)$ is odd. The sum over l can now be immediately performed. Requiring that the argument of the factorial is non-negative gives the limits of the final sum over k as

$$\sum_k \rightarrow \sum_{k=\max(0,(n-m)/2)}^{[m/2]},$$

where [ ] denotes the integral part. Now, for $n \geq m$,

$$\frac{m!}{(m-2k)!}=2^{2k}\left[-\frac{m}{2}\right]_k\left[-\frac{m}{2}+\frac{1}{2}\right]_k$$

so that

$$I(m,n,a,b)=\frac{n!}{[(n-m)/2]!}(b^2-1)^{(n-m)/2}(2ab)^m\,{}_2F_1\left[-\frac{m}{2},-\frac{m}{2}+\frac{1}{2};\frac{n-m}{2}+1;x\right], \tag{A10}$$

where $x=[(a^2-1)(b^2-1)]/a^2b^2$ and ${}_2F_1(\alpha,\beta;\gamma;x)$ is a generalized hypergeometric series but is equivalent to $F(\alpha,\beta;\gamma;x)$ the hypergeometric series.[8(b)] An analogous result holds for $m \geq n$ by interchanging m and n and a and b.

We now let $a=[2/(1+f^2)]^{1/2}$ and $b=f[2/(1+f^2)]^{1/2}$ so that $a^2-1=(1-f^2)/(1+f^2)$, $b^2-1=(f^2-1)/(1+f^2)$, and $x=-[(f^2-1)^2/4f^2]$. Since x is negative it is possible to transform the result to one in terms of an associated Legendre function by noting that[8(b)]

$${}_2F_1\left[\frac{-m}{2},\frac{-m}{2}+\frac{1}{2};\frac{n-m}{2}+1;\frac{-(f^2-1)^2}{4f^2}\right]$$
$$=2^{(n-m)/2}\Gamma\left[\frac{n-m}{2}+1\right]\left[\frac{2f}{1-f^2}\right]^{(n-m)/2}\left[\frac{1+f^2}{2f}\right]^{(n+m)/2}P^{(m-n)/2}_{(m+n)/2}\left[\frac{2f}{1+f^2}\right]. \tag{A11}$$

Therefore,

$$A_{m,n}=\left[\frac{n!}{m!}\right]^{1/2}P^{(m-n)/2}_{(m+n)/2}\left[\frac{2f}{1+f^2}\right],\quad m\geq n \tag{A12a}$$

$$=\left[\frac{m!}{n!}\right]^{1/2}(-1)^{(m-n)/2}P^{(n-m)/2}_{(n+m)/2}\left[\frac{2f}{1+f^2}\right],\quad n\leq m\,. \tag{A12b}$$

These formulas are actually equivalent since $P_n^{-m}(x)=[(n-m)!]/[(n+m)!](-1)^mP_n^m(x)$.

---

*Present address: Daresbury Laboratory, Science Research Council, Daresbury, Warrington WA44AD, United Kingdom.

[1] L. Dobrzynski and A. A. Maradudin, Phys. Rev. B 6, 3810 (1972).
[2] L. C. Davis, Phys. Rev. B 14, 5523 (1976).
[3] J. Sanehez-Dehesa and F. Flores, Solid State Commun. 35, 815 (1980).
[4] A. Eguiluz and A. A. Maradudin, Phys. Rev. B 14, 5526 (1976).
[5] G. C. Aers, A. D. Boardman, and B. V. Paranjape, J. Phys. F 10, 53 (1980).
[6] J. C. Ashley and L. C. Emerson, Surf. Sci. 41, 615 (1974).
[7] J. L. Powell and B. Crasemann, Quantum Mechanics (Addison-Wesley, Reading, Mass., 1962), p. 134.
[8] *Handbook of Mathematical Functions*, edited by M. Abramowitz and I. A. Stegun, Natl. Bur. Stand.,

Appl. Math. Ser. 55 (U.S. GPO, Washington, D.C., 1972), (a) p. 686; (b) 556:15.1.1; 562:15.4.11.
[9]The simplification of λ_{mn} uses recurrence relations for Legendre functions on the cut. The relations in Abramowitz and Stegun refer to the function off the cut, so they are not applicable. The equations on p. 161 of Vol. III of the *Bateman Manuscript Project, Higher Transcendental Functions* (McGraw-Hill, New York, 1954) were used instead.